J Orthop Sci (1999) 4:431–438

Journal of
Orthopaedic Science

Quantitative analysis of three-dimensional complexity and connectivity changes in trabecular microarchitecture in relation to aging, menopause, and inflammation

Taro Mawatari[1], Hiromasa Miura[1], Hidehiko Higaki[2], Kosaku Kurata[3], Takaaki Moro-oka[1], Teruo Murakami[3], and Yukihide Iwamoto[1]

[1] Department of Orthopaedic Surgery, Graduate School of Medical Sciences, Kyushu University, Fukuoka 812-8582, Japan
[2] Department of Mechanical Engineering, Faculty of Engineering, Kyushu Sangyo University, Fukuoka 812-8503, Japan
[3] Department of Intelligent Machinery and Systems, Faculty of Engineering, Kyushu University, Fukuoka 812-8581, Japan

Abstract: There are several types of bone loss besides that associated with normal aging, eg, that associated with the menopause, and that associated with chronic inflammation, and these are considered to be caused by different mechanisms. The microarchitecture that results from these different bone-loss mechanisms would not be the same. The purpose of this study was to investigate differences in the three-dimensional trabecular microarchitecture in various types of osteopenia, using microcomputed tomography (Micro-CT). Thirty-five Fisher 344 rats were divided into five groups (control, young, senile, ovariectomized [OVX], and inflammation-mediated osteopenia [IMO]) and distal femoral metaphysis was scanned by Micro-CT to nondestructively acquire a 3-D CT stack consisting of 50 consecutive slices at a spatial resolution of 26 μm. The volume of interest, consisting of the secondary spongiosa, was prepared to analyze the 3-D trabecular microarchitecture. A parametric analysis was carried out using bone volume fractions, fractal dimensions, and the first Betti number in order to quantitatively express the mass, complexity, and connectivity of the trabecular microarchitecture. Complexity tended to decrease with age, and decreased significantly in estrogen deficiency-induced and inflammation-mediated osteopenia. Connectivity did not appear to change with aging, but was significantly decreased in estrogen deficiency-induced and inflammation-mediated osteopenia. There was no significant difference between the OVX and the IMO groups.

Key words: postmenopausal osteoporosis, age-related osteopenia, inflammation-mediated osteopenia, fractal dimension, connectivity

Offprint requests to: H. Miura, 3-1-1 Maidashi, Higashi-ku, Fukuoka 812-8582, Japan
Received for publication on Dec. 3, 1998; accepted on May 21, 1999

Introduction

There are several types of bone loss besides normal aging, such as postmenopausal osteoporosis, inflammation-mediated osteopenia (IMO),[15,20] and corticosteroid-induced osteoporosis.[26] Since each of these types of bone loss seems to be caused by different mechanisms, the microarchitecture that results from these different bone-loss mechanisms would not be the same. However, structure is not predicted by the quantity of mineralized bone; namely, bone mineral density (BMD), and few attempts have been made so far to quantitatively compare the three-dimensional (3-D) microarchitecture with respect to age- and postmenopausal- and inflammation-related bone loss.

Both trabecular bone loss and architectural deterioration have been considered to cause an increased incidence of osteoporotic fracture.[6] Accurate evaluation of microarchitecture requires accurate 3-D information on trabecular bone, since the trabecular architecture is anisotropic. For many reasons, conventional histomorphometry is not sufficient for gathering 3-D information about trabecular bone. First, destruction, shrinking, and uneven staining in the processing of histologic sections are, to a certain extent, unavoidable. Furthermore, defects in section grinding cause low resolution in the direction perpendicular to the slice. Finally, separated sections lose their axis of reference relative to each other. All of these factors make it difficult to acquire volume data. Recently, a number of methods for 3-D analysis have been reported, including microcomputed tomography (Micro-CT),[13,21] high-resolution magnetic resonance imaging,[16] a serial sectioning procedure,[24] and X-ray tomographic microscopy using synchrotron radiation sources.[12] These methods make 3-D microstructural analysis much easier.

The importance of structural changes in trabecular bone and the relation of these changes to the biomechanical competence of trabecular bone has been

stressed by Parfitt,[27] mainly because the loss of structural connectivity is an irreversible process as new lamellar bone can only be added to existing surfaces. Fractal dimension and structural connectivity have been proposed as useful parameters to explain the microarchitectural changes in trabecular bone.[7,8,23,25]

The notion of "fractal" was originally described by Mandelbrot,[18] and the self-similarity between complex structures in nature and a certain class of mathematical objects was called "fractal". A natural fractal exhibits statistical self-similarity but only over a limited range of scale, and fractal analysis has been applied to a number of biologic structures, including the bronchial tree and the vascular network.[5] The fractal dimension describes how an object occupies space and is related to the complexity of its structures. When applied to trabecular bone, the fractal dimension provides additional information on structure and mechanical properties.

Connectivity has been considered to be the parameter most affected by osteoporotic changes. The intuitive concept of connectivity was developed as a basic topological method for quantifying the connectivity of cancellous bone by Feldkamp et al.,[8] Odgaard and Gundersen,[25] and Gundersen et al.[9] Recently, more accurate estimation of connectivity, using the first Betti number, has been done based on the Euler characteristic calculated by the Feldkamp method.[8]

Although several groups have reported the application of fractal and topological analyses to the study of cancellous bone,[19] few of them have compared the 3-D trabecular architecture in pathologic status with that in normal aging. We used microcomputed tomography for the assessment of 3-D microstructure by reconstructed volume information from consecutive slice images, and established a method for the quantitative assessment of 3-D complexity and connectivity, using, respectively, the fractal dimension and the first Betti number (see definition under "Topological analysis").

The purpose of this study was to explore morphologic changes in the trabecular microarchitecture in relation to aging, menopause, and inflammation, using animal models.

Materials and methods

Experimental procedures

We obtained 35 female breeder Fisher 344 rats, aged 11 weeks and weighing 160–190 g (Seac Yoshitomi, Fukuoka, Japan). After a 1-week acclimation period, the animals were randomly divided into five groups, as described below ($n = 7$/group), and were kept in pairs at 22°C with a 12/12 h light/dark cycle until they were killed. The *control* group consisted of 21-week-old rats. The *young* group were 12-week-old rats, representing rats younger than 21 weeks, which should be fertile. The *senile* group were 2-year-old rats. The *OVX* group were 21-week-old rats ovariectomized bilaterally at age 13 weeks, as a postmenopausal osteoporosis model. The *IMO* group were 21-week-old rats injected seven times, at weekly intervals, before termination, with 600 mg of magnesium silicate suspended in 1.0 ml saline subcutaneously, as an inflammation-mediated osteopenia (IMO) model.

After the rats were killed, the right femur was excised, defleshed, and fixed in 70% ethanol, and metaphyseal trabecular bone of the distal femur, with the exclusion of the area situated within 1.085 mm from the epiphyseal growth plates, to exclude the primary spongiosa, was scanned by Micro-CT (MCT-12505MF; Hitachi Medical, Kashiwa, Japan; Fig. 1) to nondestructively acquire a 3-D CT stack consisting of 50 consecutive slices at a spatial resolution of 0.026 mm. This Micro-CT uses a microfocus X-ray tube as a source, an image intensifier as a 2-D detector, and enables the creation of a high-resolution CT image with a maximum resolution of 0.026 mm (Fig. 2). The following CT setting was used: effective energy, 40 keV; slice thickness, 0.020 mm; pixel matrix, 480 × 480; pixel size, 0.026 mm; magnification, ×10. The height level of measurement was decided accurately using the height adjustment function of the Micro-CT under fluoroscopic imaging.

All procedures performed on the rats were approved by the Institutional Animal Care and Use Committee at the Kyushu University at Fukuoka and complied with the *American Journal of Physiology* guidelines.

Fig. 1. Microcomputed tomography (Micro-CT; MCT-12505MF; Hitachi Medical Corporation, Kashiwa, Japan)

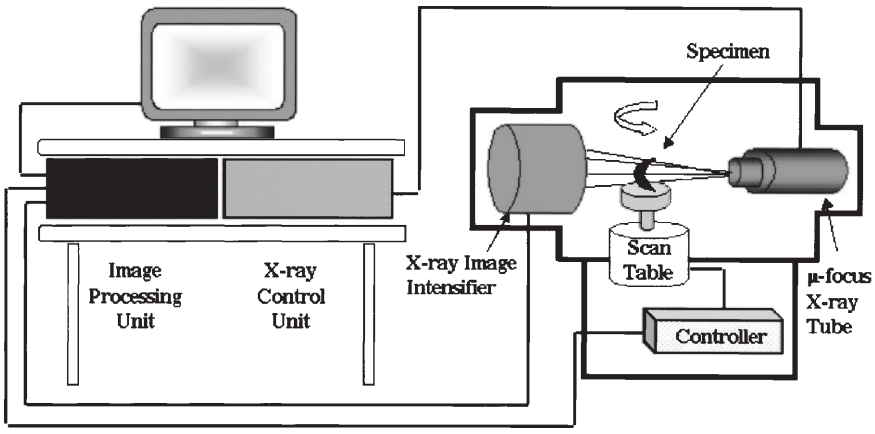

Fig. 2. Construction of MCT-12505MF

Data analysis

Raw volume data were transferred to a personal Computer (Power Macintosh 8100/80, Apple Computer, Cupertino, CA, USA) and all of the parametric analyses were done using custom-made software. All the gray-value slice images were then noise-eliminated, segmented, and transformed to binary images, which included a local thresholding procedure.[13] Preliminary experiments on the rat trabecular bone were specifically designed to select the correct threshold value. The proximal metaphysis of the rat tibia was scanned by Micro-CT, and the same sample data were analyzed several times by changing parameters. Finally, fixed parameter values in this analysis were determined by comparing the bone volume fraction derived from the Micro-CT image with that derived from the histologic section of approximately the same plane. All specimens were segmented using the same parameter setting, and the relative comparisons were done under equal conditions. Then, by compilation of consecutive 2-D slice images, a 3-D reconstructed data-set providing a nominal isotropic voxel size of 20 μm was obtained after appropriate interpolation.

The volume of interest (VOI) for parametric analysis was that of rectangular trabecular bone columns (Fig. 3; $3.12 \times 3.12 \times 1.00\,mm^3$) situated at the center of the distal metaphysis. When extracting the VOI, rotational orientation was arranged in the same alignment.

Parametric analysis was done using bone volume fractions, fractal dimension, and the first Betti number for the quantitative analysis of microarchitectural changes in trabecular bone in each model.

Bone volume fraction

Bone volume fraction (***BV/TV***, %) is a measure of the volume of trabecular bone per total volume of analysis

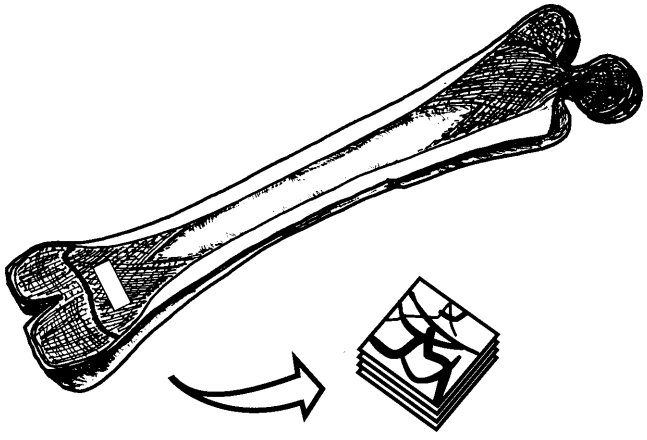

Fig. 3. The volume of interest consisted of rectangular columns ($3.12 \times 3.12 \times 1.00\,mm^3$) of secondary spongiosa situated at the center of the distal metaphysis of the right femur

in the column, which means the density of voxels representing bone.

Fractal analysis

The fractal dimensions of the trabecular columns were measured using a 3-D box-counting method implemented on the personal computer. The fractal analysis software repeatedly applied cubes with varied side lengths to the binarized volumes, counting the number of cubes which contained the surface. Log-log graphs were plotted of the reciprocal of the side length of the cube (***d***) against the number of surface-containing cubes (***N(d)***). The gradient of linear segments of these graphs was calculated using the least-squares method of regression. The figure for each rat demonstrated a strict linear correlation between log ***d*** and log ***N(d)*** on a logarithmic graph, which means that the trabecular organization of the bone was fractal. The fractal

dimension was calculated from the absolute value of the gradient of the line.

Topological analysis

Topological analysis was done using the first Betti number, $\beta\boldsymbol{1}$, which is defined as the topological connectivity estimated from an enumeration of the number of closed loops in the analyzed volume.[14] At first, on the purified volumes, both the trabecular bone that was continuously interconnected and any isolated structures that were disconnected from the surrounding cortical bone and trabecular structure were identified and labeled. Then, a direct measure of $\beta\boldsymbol{0}$ and $\beta\boldsymbol{2}$, the topological variables that quantify both the number of isolated bone fragments and the number of imbedded pores, was provided. Next, by using the Feldkamp algorithm[8] on purified volumes, the Euler characteristic χ was calculated. Finally, $\beta\boldsymbol{1}$ was calculated using the Euler-Poincaré formula:

$$\beta\boldsymbol{1} = \beta\boldsymbol{0} - \chi + \beta\boldsymbol{2}$$

which was then normalized over the total analysis volume and the connectivity density, $\beta\boldsymbol{1}/\boldsymbol{TV}$ ($1/mm^3$), was referred for relative comparison.

3-D Rendered image

3-D rendered images of trabeculae were obtained by surface-rendering methods, using the AVS Medical Viewer (KGT, Tokyo, Japan) installed on a workstation (ONYX2; Silicon Graphics, Mountain View, CA, USA).

Reproducibility study

To determine the inter-rater and intra-rater reliability of our analysis procedure from the derived data, three experienced raters analyzed 10 distal femoral scans that were randomly selected from 35 study specimens. The raters adjusted the rotational alignment of the specimen and identified the VOI consisting of secondary spongiosa, and then each structural index was calculated. Ten scans were analyzed to determine inter-rater reliability, and the analyses were repeated on the same 10 scans after 9 days to determine intra-rater reliability.

Statistical analysis

Using the original and repeat measurements, reproducibility can be assessed by repeated-measure random effects analysis of variance (ANOVA) models. We analyzed the inter-rater and intra-rater data separately. We fitted two-factor models, including rater in addition to subject, using a BMDP software package (BMDP2V; BMDP Statistical Software, Los Angeles, CA, USA). From these models we estimated the inter-rater reliability coefficient and the intra-rater reliability coefficient.

Statistical analyses of **BV/TV**, fractal dimension, and the first Betti number were performed with the Stat View software package (Stat View, Abacus Concepts, Berkeley, CA, USA). Analysis of variance (Fisher's PLSD multiple comparison procedure) at the $P = 0.05$ level was used to examine the differences between each group. Pearson's correlation coefficient was calculated for fractal dimension and **BV/TV** or the first Betti number, as well as between the first Betti number and **BV/TV**.

Results

All animals tolerated the experiment without complications. Intra-rater reliability for scans measured in 9 days averaged 92% for **BV/TV**, fractal dimension, and the first Betti number. Reliability between raters ranged from 83.74% for **BV/TV** to 95.52% for the first Betti number (Table 1).

Three-dimensional surface-rendered images representing each group are shown in Fig. 4. In the *control* group, the distinct platelike structure of bone can easily be seen and the connecting rods are well developed. A more complicated microarchitecture was seen in the *young* group, while in the *senile* group the plates were still present but scarce. In contrast, in the osteoporosis (*OVX* and *IMO*) groups, the platelike structure had

Table 1. Inter-rater and intra-rater reliability of Micro-CT scan analyses

	BV/TV	Fractal dimension	First Betti number
σ^2_{rater}: Between rater variance	2.7	0.0	1.6
$\sigma^2_{subject}$: Between subject variance	56.5	0.0	3405.1
Inter-rater reliability	83.7%	90.8%	95.5%
Intra-rater reliability	95.8%	92.4%	98.7%

BV, Volume of trabecular bone; **TV**, total volume of analysis; Micro-CT, microcomputed tomography

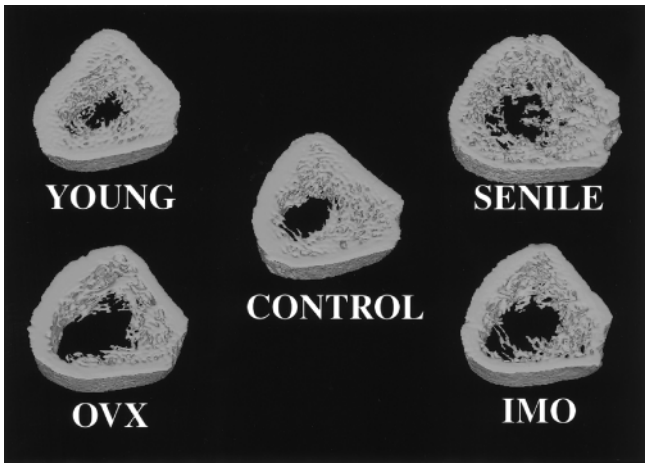

Fig. 4. Three-dimensional rendered images of trabecular bone (×10). *OVX*, Ovariectomized postmenopausal osteoporosis model; *IMO*, inflammation mediated-osteopenia model

partially resolved into a rodlike structure, with many of the connecting rods missing.

The results of parametric analyses of **BV/TV**, fractal dimension, and the first Betti number are shown in Fig. 5. The fractal dimension tended to decrease with age, and decreased significantly in the osteoporosis groups. **BV/TV** and the first Betti number did not appear to change with age, but decreased significantly in the osteoporosis groups. These findings agreed with the rendered images. Figure 6 shows the correlation between fractal dimension and **BV/TV** or the first Betti number as well as between the first Betti number and **BV/TV** in each group. All the correlations between fractal dimension and **BV/TV**, fractal dimension and the first Betti number, and between the first Betti number and **BV/TV** were significant.

Discussion

Three-dimensional visual assessment of the rendered volumes allowed recognition of microarchitectural changes in cancellous bone. The surface-rendered model revealed the trabecular microarchitecture in detail, which allows better understanding of the morphometric changes of trabecular bone in relation to aging, menopause, and inflammation.

The fractal dimension, which reflects complexity and space occupancy, appeared to decrease with aging or osteoporotic status. Our results, calculated by a 3-D box-counting algorithm, agree with the trend in the 2-D analysis of Weinstein and Majumdar,[30] who obtained values of 1.60 for the fractal dimension of normal bone and 1.27 for osteoporotic bone. Several methods have

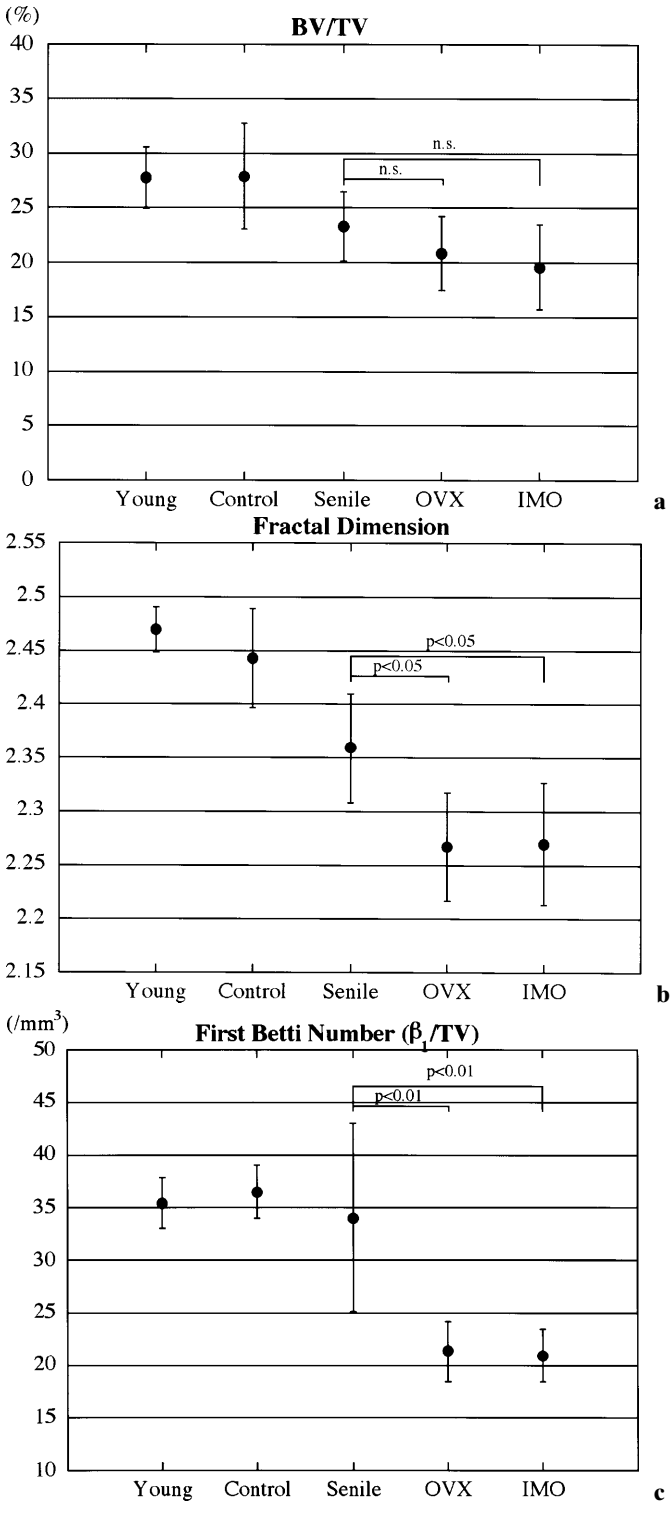

Fig. 5a–c. Results for each parameter measured. **a** Bone volume fraction (volume of trabecular bone; ***BV*** / total volume of analysis; ***TV***), **b** Fractal dimension. **c** the first Betti number. *OVX*, Ovariectomized postmenopausal osteoporosis model; *IMO*, inflammation-mediated osteopenia model

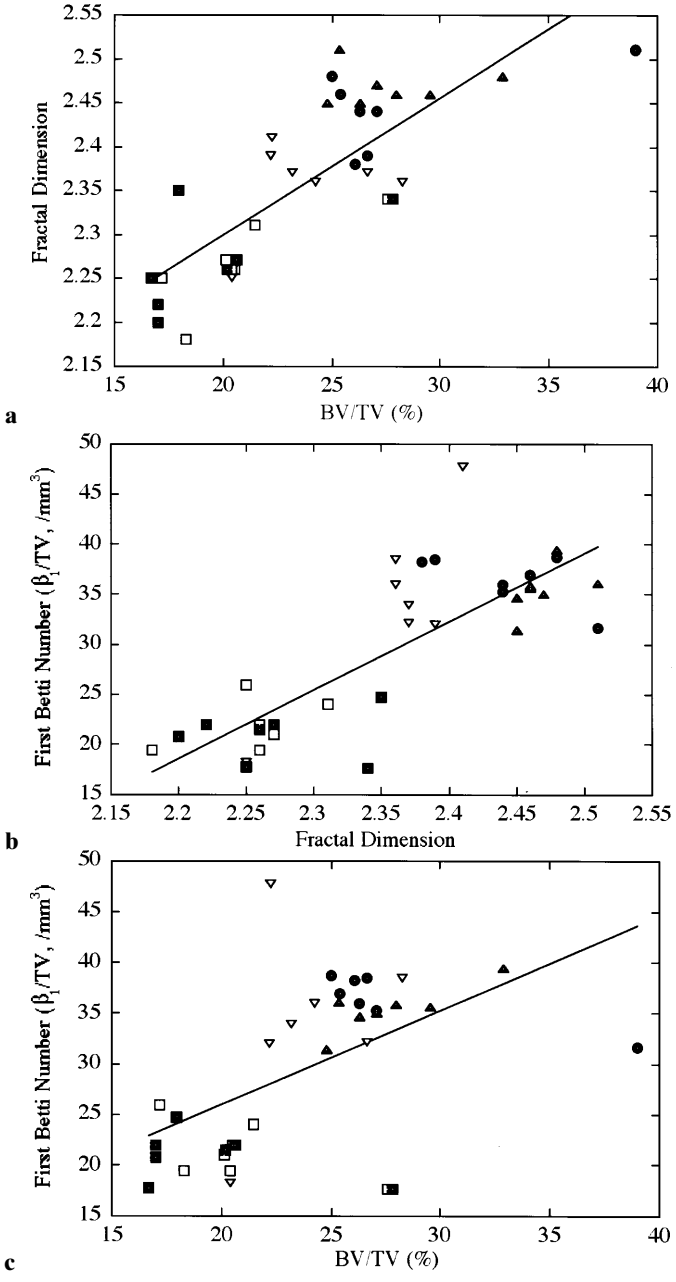

Fig. 6a–c. Correlation between parameters. **a** Fractal dimension vs bone volume fraction. **b** Fractal dimension vs the first Betti number. **c** The first Betti number vs bone volume fraction. *OVX*, Ovariectomized postmenopausal osteoporosis model (*open squares*); *IMO*, inflammation-mediated-osteopenia model (*closed squares*). *Closed dots*, control group; *closed triangles*, young group; *open triangles*, senile group. **a** $r = 0.79$; **b** $r = 0.54$; **c** $r = 0.78$

been proposed for determining the fractal dimension, including the box-counting algorithm,[7,17,30] surface-area techniques using radiographs,[3] and power spectrum representations of 2-D Fourier transforms of radiographs.[2,29] When the fractal dimension is determined from projected 2-D radiographs, interpretation of the results is very difficult because the images are composed of many trabecular structures superimposed in the same region. For example, both the fractal dimension measured from radiographs of peridental alveolar bone, as reported by Ruttimann et al.,[29] and the fractal dimension measured from calcaneus radiographs, as reported by Benhamou et al.,[1] increase as the bone becomes coarse, while the fractal dimension measured from radius radiographs, as reported by Khosrovi et al.,[10] shows the opposite trend. Caligiuri et al.[3] reported that the fractal dimension, as measured from lumbar spine radiographs, increased with aging, while Berry et al.[2] demonstrated an increase in the fractal dimension with bone dissolved in acid. Thus, interpretation of fractal dimensions calculated by different methods may be complicated, and 3-D analysis such as the 3-D box-counting method could be the better choice.

The first Betti number, compared with the Euler characteristic, has been suggested to provide a more detailed numerical description of topological properties.[4,9,25] In particular, when topological properties are evaluated from limited VOIs rather than from whole bone, use of the first Betti number is preferable. The reason for this is that $\beta\boldsymbol{0}$ is greater than 1 because the connection was cut at the margin of the extracted VOI and isolated islands of bone may exist, while $\beta\boldsymbol{0}$ is assumed to be a constant, (i.e., $\beta\boldsymbol{0} = 1$). In other words, all trabeculae are assumed to form only one connected part when the Euler characteristic is calculated. The first Betti number, like the Euler number, is a topological quantity and as such carries no information regarding the efficacy of the positions of connections, the size of connections, or the strength of the material that makes up the connections. Hence, by itself, it cannot be expected to be an index of extrinsic mechanical performance. On the other hand, it appears promising as a means of distinguishing between structures that are equivalent according to more primary measures, such as total bone mass, although the precise relationship between density, structure, and mechanical properties is still under investigation.

There are many distinctions between postmenopausal and age-related osteoporosis. The proposed mechanism of this estrogen deficiency-induced bone loss is fenestration and complete removal of trabeculae as a result of increased remodeling activity.[28] In agreement with this concept, the fractal dimension and the first Betti number, which quantitatively describe 3-D complexity and connectivity changes in the trabecular microarchitecture, were decreased significantly in osteoporosis models. As far as the relationship among the mass, complexity, and connectivity of the trabecular

bone is concerned, all these parameters were significantly correlated with each other.

Inflammation-mediated osteopenia has been proposed to develop independently of parathyroid hormone and vitamin D metabolites,[15,20] and is considered to be different from estrogen deficiency-induced osteopenia. Although we predicted that there would be differences in the morphometric changes between the OVX and the IMO groups, there was no significant difference between these groups in the fractal dimension and the first Betti number in our morphometric analysis of trabecular bone. We could not distinguish any differences by the appearance of reconstructed images. We were not dealing with corticosteroid-induced osteopenia in this study, but it is interesting to note that the pattern of bone loss with corticosteroids has been considered to lead to a thinning of the trabecular plates without a change in the connectivity.

There are several limitations to this study. First, we chose the distal femoral metaphysis, which is rich in cancellous bone, as the imaging site, although a more common histologic sampling site is the proximal tibia or the vertebrae. While the bone mass of the distal femoral metaphysis of rats is known to decrease in osteoporotic status, other portions should be surveyed, because morphometric changes in osteoporosis vary depending on the anatomic location. Further, Kimmel[11] has suggested that the age of female rats as a model of the adult human female skeleton should be $\geq$7 months to exclude complications associated with endochondral ossification. Hence, further studies using older rat models should be performed.

Second, we did not analyze distorted whole secondary spongiosa, but rather, a VOI extracted from the whole bone. Therefore, we verified the reproducibility of 3-D parameters. These parameters were accomplished by accurate settings of measurement height level using the height measurement function of Micro-CT and by precise VOI definitions, which were uniquely identified after adjustment of rotational orientation.

Finally, Micro-CT provided a satisfactory noninvasive assessment of consecutive slice images corresponding reasonably well to the histologic sections, although a resolution of 0.026 mm seems to be the lowest resolution level for studies in small animals such as rats, in which the trabecular width averages approximately 0.050 mm and trabecular separations average 0.150 mm or less.[12] It is important to realize that at this resolution, the slice thickness is the same level as the trabecular dimension, and because of this resolution, 3-D measures will be limited. Hence, one should keep in mind that data calculated from binarized images are relative rather than absolute, and relative comparisons are important. However, despite the limited resolution, relative differences in the architecture between age-, postmenopausal-, and inflammation-related bone loss were revealed. Although the use of computed tomography to achieve a resolution below 0.100 mm in human subjects in vivo may be difficult because of dose considerations,[22] there are several encouraging reports of high-resolution magnetic resonance imaging techniques[16] which may have the potential for such high resolution; the quantitative parametric analysis presented in this article should be useful for future studies.

In conclusion, using rat models of estrogen deficiency-induced, inflammation-mediated, and age-related osteopenia, we quantitatively demonstrated 3-D complexity and connectivity changes in relation to menopause, inflammation, and aging, which changes agreed with the visual assessment of 3-D rendered volume images. These quantitative parametric analyses of complexity and connectivity may be useful both for distinguishing osteoporotic from normal bone structure, and for evaluating different therapeutic regimens.

Acknowledgments. The authors wish to thank Naoko Kinukawa, M.S. for technical assistance in the statistical analyses. This work was supported in part by a Grant-in-Aid for General Scientific Research (Grant no. 08457392) from the Ministry of Education, Science and Culture, Japan.

References

1. Benhamou CL, Lespessailles E, Jacquet G, et al. Fractal organization of trabecular bone images on calcaneus radiographs. J Bone Miner Res 1994;9:1909–18.
2. Berry JL, Towers JD, Webber RL, et al. Change in trabecular architecture as measured by fractal dimension. J Biomech 1996; 29:819–22.
3. Caligiuri P, Giger ML, Favus M. Multifractal radiographic analysis of osteoporosis. Med Phys 1994;21:503–8.
4. Compston JE. Connectivity of cancellous bone: assessment and mechanical implications [editorial]. Bone 1994;15:463–6.
5. Cross SS. The application of fractal geometric analysis to microscopic images. Micron 1994;25:101–13.
6. Cummings SR, Kelsey JL, Nevitt MC, et al. Epidemiology of osteoporosis and osteoporotic fractures. Epidemiol Rev 1985; 7:178–208.
7. Fazzalari NL, Parkinson IH. Fractal dimension and architecture of trabecular bone. J Pathol 1996;178:100–5.
8. Feldkamp LA, Goldstein SA, Parfitt AM, et al. The direct examination of three-dimensional bone architecture in vitro by computed tomography. J Bone Miner Res 1989;4:3–11.
9. Gundersen HJG, Boyce RW, Nyengaard JR, et al. The conneulor: unbiased estimation of connectivity using physical disectors under projection. Bone 1993;14:217–22.
10. Khosrovi PM, Kahn AJ, Genant HK, et al. Characterization of trabecular bone structure from radiographs using fractal analysis. J Bone Miner Res 1994;9:S156.

11. Kimmel DB. Quantitative histologic changes in the proximal tibial growth cartilage of aged female rats. Cells Materials 1991; Suppl 1:11–18.
12. Kinney JH, Lane NE, Haupt DL. In vivo, three-dimensional microscopy of trabecular bone. J Bone Miner Res 1995;10:264–70.
13. Kuhn JL, Goldstein SA, Feldkamp LA, et al. Evaluation of a microcomputed tomography system to study trabecular bone structure. J Orthop Res 1990;8:833–42.
14. Lane NE, Thompson JM, Strewler GJ, et al. Intermittent treatment with human parathyroid hormone (hPTH[1–34]) increased trabecular bone volume but not connectivity in osteopenic rats. J Bone Miner Res 1995;10:1470–7.
15. Lempert UG, Minne HW, Fleisch H, et al. Inflammation-mediated osteopenia (IMO): no change in bone resorption during its development. Calcif Tissue Int 1991;48:291–2.
16. Majumdar S, Kothari M, Augat P, et al. High-resolution magnetic resonance imaging: three-dimensional trabecular bone architecture and biomechanical properties. Bone 1998;22:445–54.
17. Majumdar S, Weinstein RS, Prasad RR. Application of fractal geometry techniques to the study of trabecular bone [published erratum appears in Med Phys 1994 Mar;21(3):491]. Med Phys 1993;20:1611–19.
18. Mandelbrot BB. Fractals: form, chance, and dimension. San Francisco: WH Freeman; 1977.
19. Mellish RWE, Garrahan NJ, Compston JE. Age-related changes in trabecular width and spacing in human iliac crest biopsies. Bone Miner 1989;6:331–8.
20. Minne HW, Pfeilschifter J, Scharla S, et al. Inflammation-mediated osteopenia in the rat: a new animal model for pathological loss of bone mass. Endocrinology 1984;115:50–4.
21. Müller R, Hahn M, Vogel M, et al. Morphometric analysis of noninvasively assessed bone biopsies: comparison of high-resolution computed tomography and histologic sections. Bone 1996;18:215–20.
22. Müller R, Hildebrand T, Häuselmann HJ, et al. In vivo reproducibility of three-dimensional structural properties of noninvasive bone biopsies using 3D-pQCT. J Bone Miner Res 1996;11:1745–50.
23. Odgaard A. Three-dimensional methods for quantification of cancellous bone architecture. Bone 1997;20:315–28.
24. Odgaard A, Andersen K, Ullerup R, et al. Three-dimensional reconstruction of entire vertebral bodies. Bone 1994;15:335–42.
25. Odgaard A, Gundersen HJG. Quantification of connectivity in cancellous bone, with special emphasis on 3-D reconstructions. Bone 1993;14:173–82.
26. Olbricht T, Benker G. Glucocorticoid-induced osteoporosis: pathogenesis, prevention and treatment, with special regard to the rheumatic diseases. J Intern Med 1993;234:237–44.
27. Parfitt AM. Trabecular bone architecture in the pathogenesis and prevention of fracture. Am J Med 1987;82:68–72.
28. Parfitt AM, Mathews CHE, Villanueva AR, et al. Relationships between surface, volume, and thickness of iliac trabecular bone in aging and in osteoporosis. Implications for the microanatomic and cellular mechanisms of bone loss. J Clin Invest 1983;72:1396–409.
29. Ruttimann UE, Webber RL, Hazelrig JB. Fractal dimension from radiographs of peridental alveolar bone. A possible diagnostic indicator of osteoporosis. Oral Surg Oral Med Oral Pathol 1992;74:98–110.
30. Weinstein RS, Majumdar S. Fractal geometry and vertebral compression fractures. J Bone Miner Res 1994;9:1797–802.